INTERNATIONAL JOURNAL OF ELECTRICAL ENGINEERING & TECHNOLOGY (IJEET)

ISSN 0976 – 6545(Print)
ISSN 0976 – 6553(Online)
Volume 4, Issue 4, July-August (2013), pp. 287-295
© IAEME: www.iaeme.com/ijeet.asp
Journal Impact Factor (2013): 5.5028 (Calculated by GISI)
www.jifactor.com

IJEET
©IAEME

NOVEL DIFFERENTIAL LINEAR ELECTROSTATIC MOTOR

Saad Tapuchi, Arie Shenkman and Dmitry Baimel

Department of Electrical and Electronics Engineering, Shamoon College of Engineering, Beer Sheva, Israel

ABSTRACT

The paper proposes a new type of linear electrostatic motor operated on a principle of the electric field effect on dielectric material. The proposed motor has a simple structure that simplifies the production process. Furthermore, the proposed motor has advanced motion control options that allow precise control of velocity and position profiles. Extensive simulation results of the proposed motor at different operation modes are presented and analyzed. The simulation results demonstrate proposed control methods and show the practicability of the motor.

Key words: Electrostatic motor, linear motor, electric field, motion control.

I. INTRODUCTION

Today, most of the electrical machines operate on the principle of magnetic field effect at which the electric energy is converted into mechanical energy and vice versa. The magnetic field is produced by the current flowing in the stator and rotor coils.

On the other hand, it is also possible to construct electrical machines that operate on the electric field principle, where the electrical energy is stored in an electric field [1-2]. It is known that the electric and the magnetic fields are always linked to each other and it is impossible to separate them. However, the electric field in the electromagnetic machines is much weaker than the magnetic field, and, practically, is negligible.

The electric machines operated on the electric field principle would have mechanical structure based on capacitors, while the mechanical structure of the electromagnetic machines is based on the inductors. Today, the development of the electromagnetic machines has reached the most advanced state, while the electric field machines (capacitor machines) remained somehow ignored. The reason is low electric permittivity- ε of most dielectric materials. However, recently, new dielectric materials have been developed. These materials are based on compressed ceramic powder and possess relatively high electric permittivity of up to $\varepsilon_r = 1.7*10^4$. The dielectric materials with such a high electric permittivity can increase motor's torque.

There are a lot of electrostatic motors topologies [3-6]. The most common configurations are film motors [7-10], micro-motors [11-13], linear inchworm motors [14-15], comb motors [16-18] and wobble motors [19-20]. These topologies are well known in the literature and their disadvantage is rather complex structure and sophisticated control. The proposed motor overcomes these disadvantages.

Section 2 presents the proposed motor. Section 3 presents different control methods of the motor. The control methods are simulated, analyzed. The conclusions are presented in section 4.

II. THE PROPOSED DIFFERENTIAL ELECTROSTATIC MOTOR

The proposed motor is based on the principle of dielectric slab insertion between capacitor plates. The voltage application to the capacitor plates will generate force that will drag the dielectric slab into the capacitor until the plates will be completely filled by the slab (see Fig. 1).

The depth of slab insertion into the plates is defined as 'x'. Therefore, the total capacitor can be seen as two capacitors connected in parallel: the first capacitor with air as the dielectric material (electric permittivity of ε_0) and the second capacitor with the slab as dielectric material (relative electric permittivity of $\varepsilon_r = 1.7*10^4$). Therefore, the total capacitance can be calculated by eq. (1).

$$C_T = C_1 + C_2 = \frac{\varepsilon_0 * (l-x) * b}{d} + \frac{\varepsilon_0 * \varepsilon_r * x * b}{d} = \frac{\varepsilon_0 * b}{d}(l - x + x * \varepsilon_r) \qquad (1)$$

The energy stored in this capacitor would be:

$$W = \frac{C * V^2}{2} = \frac{\varepsilon_0 * b}{d}(l - x + x * \varepsilon_r) \ * \frac{V^2}{2} \qquad (2)$$

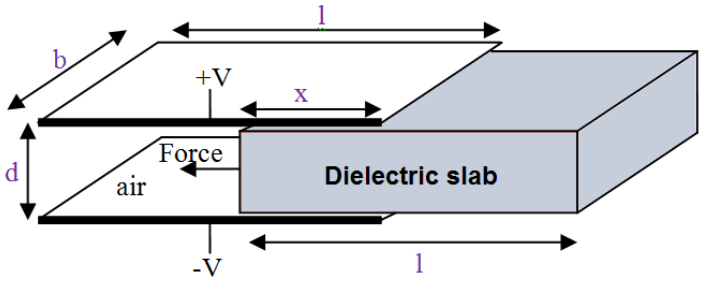

Fig. 1. Force generation that pushes dielectric slab into the capacitor until the plates are completely filled by the slab. 'd' is the distance between the plates, 'l' is the length of the dielectric slab and 'x' is the depth of the slab insertion between the plates.

This generated force can be calculated by:

$$F = \left|\frac{dW}{dx}\right| = \frac{\varepsilon_0 * b * V^2}{2 * d} * (\varepsilon_r - 1) \qquad (3)$$

For the high values of ε_r, the eq. (3) can be simplified to eq. (4):

$$F = \frac{\varepsilon_0 * \varepsilon_r * b * V^2}{2 * d} \qquad (4)$$

It can be clearly seen from eq. (5) that the generated force does not depend on the depth of the slab insertion 'x'. Even a small distance 'x' will be enough to generate the force that will drag the

slab into the capacitor plates. The proposed motor uses this principle in order to achieve bi-directional linear motion (see Fig. 2).

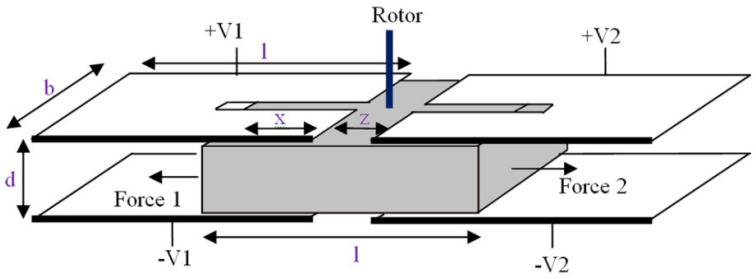

Fig. 2. The proposed differential motor

The stator of the proposed motor is constructed from two pairs of plates. The distance between the plates is defined as 'z'. The dielectric slab with welded rod at the center acts as a rotor. The rod of the rotor can enter into the upper plates through the slots. The purpose of the slots is to allow rotor's bidirectional movement. Furthermore, the slots' edges also act as mechanical stoppers for the rotor.

The slab is designed to have the same length at the length of the plates- 'l'. In order to ensure the motor's ability to generate force in both directions, the rotor's movement amplitude has to be limited in such a way that at any position of the rotor, some part of the slab will be always present in both capacitors. The rotor's movement amplitude is limited by the slots' edges and as result, at any rotor position, the depth of slab's insertion would be at least 1mm (x>=1mm). This design ensures the ability of force generation in right or left direction by application of V1 or V2 voltages.

When the voltage V1 is applied to the left capacitor, the generated force 1 will drag the rotor to the left until it will be stopped by the slots' left edge (see Fig. 3). In this case, a small part of the slab with the length of 1mm will be also present between the right pair of plates. Therefore, the application of voltage V2 to the right pair of plates will generate the force 2 that will drag the rotor to the right capacitor.

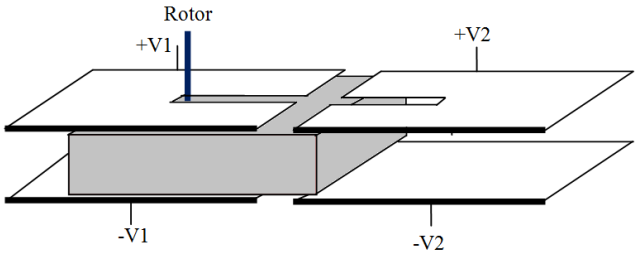

Fig. 3. The voltage V1 was applied to the left capacitor and the generated force 1 has dragged the rotor to the left.

The proposed motor is constructed with the parameters shown in Table 1. The slab is built from compressed ceramic powder with electric permittivity of $\varepsilon_r = 1.7*10^4$.

The 400V DC voltage application to one of the capacitors (left or right), would generate force of 0.32Nm.

$$F = \frac{\varepsilon_0 * \varepsilon_r * b * V^2}{2 * d} = \frac{8.86 * 10^{-12} * 17000 * 0.08 * 400^2}{2 * 0.003} = \mathbf{0.32}\ [\mathbf{Nm}].$$

The force calculation shows that the differential motor with even relatively small size (see Table 1) can generate force of 0.32 Nm. By using the motion equations, the generated force on the slab could be also defined as:

$$\boldsymbol{F = M * a} \quad (5)$$

where 'M' is the mass and 'a' is the acceleration of the slab.
The velocity can be calculated by:

$$\boldsymbol{v(t) = v_0 + \int_0^t a\,dt' = v_0 + \int_0^t \frac{F}{M} dt' = \frac{F}{M} t} \quad (7)$$

The distance of the slab's movement 'X' is calculated by:

$$\boldsymbol{X(t) = \int_0^t v dy = \int_0^t \frac{F}{M} y dy = \frac{F}{2*M} t^2} \quad (8)$$

The amplitude of the rotor's move is calculated by:

$$\boldsymbol{X_{max} = 2 * \left(\frac{l}{2} - z - 1\right) + z} \quad (10)$$

The movement amplitude of the motor with parameters from Table 1 can by calculated by using eq. (10): $\boldsymbol{X_{max} = 28mm}$.

The rotor's position is defined as zero when its rod is positioned exactly at the center of the motor i.e. at even distances z/2 from the plates (see Fig. 2). The rotor's movement to the left direction is defined as positive distance at positive velocity. The rotor's movement to the right direction is defined as negative distance at negative velocity.

Table 1. Differential motor parameters

d [mm]	B [mm]	Slab's mass [kg]	l [mm]	Z [mm]	V [v]
3	80	0.05	40	10	400

III. THE PROPOSED CONTROL METHODS FOR DIFFERENTIAL ELECTROSTATIC MOTOR

In this section, the motor's operation will be analyzed for different rotor moves and voltages types.

Eq. (5) shows that the generated force is proportional to the square of applied voltage. If the applied voltage is DC voltage, the generated force will be constant. If the applied voltage varies with time e.g. sine, triangle, or saw tooth waveforms etc., the magnitude of the generated force will also vary. Therefore, the rotor's velocity and position can be easily controlled by varying the amplitude and shape of the applied voltages V1 and V2. Moreover, closed loop control can be easily applied to the motor. As a result, precise motion control of the motor can be achieved. The proposed control methods for the motor are presented below

3.1 First method: The V1 and V2 are DC voltages

The rotor has several basic moves. The first move to be analyzed is from zero position to the X=14mm position i.e. to the left edge and backwards to the zero position (half amplitude move, see Fig. 2 and 3).

This movement is performed by application of pulsed DC voltage to the capacitors: firstly, the voltage V1 is applied to the left capacitor and afterwards, voltage V2 is applied to the right capacitor until the rotor reaches the zero position (X=0). The simulated DC voltages versus the generated forces, rotor's velocity and position are shown in Fig. 4. When the voltage V1=400V is applied to the left capacitor, the generated 'force 1' of 0.32N drags the rotor to the left (from zero to +14mm position). The rotor performs this move in 0.066sec, at average velocity of 0.21m/sec. In order to return the rotor to its initial zero position, the voltage V2=400V is applied for additional 0.066sec. When the rotor's position becomes zero, the motor control unit sets the voltage V2 to zero (see Fig. 4).

Simulation results show that in the case of DC voltages control, the rotor can achieve relatively high velocity due to constantly rising acceleration. Therefore, when fast acceleration and high speed is required, the application of DC voltages is preferable. Furthermore, the initial force is relatively high and the rotor can start to move with mechanical load. The disadvantage is that the mechanical jerk is high and immediate stopping of the rotor has a potential to cause mechanical damage to the motor.

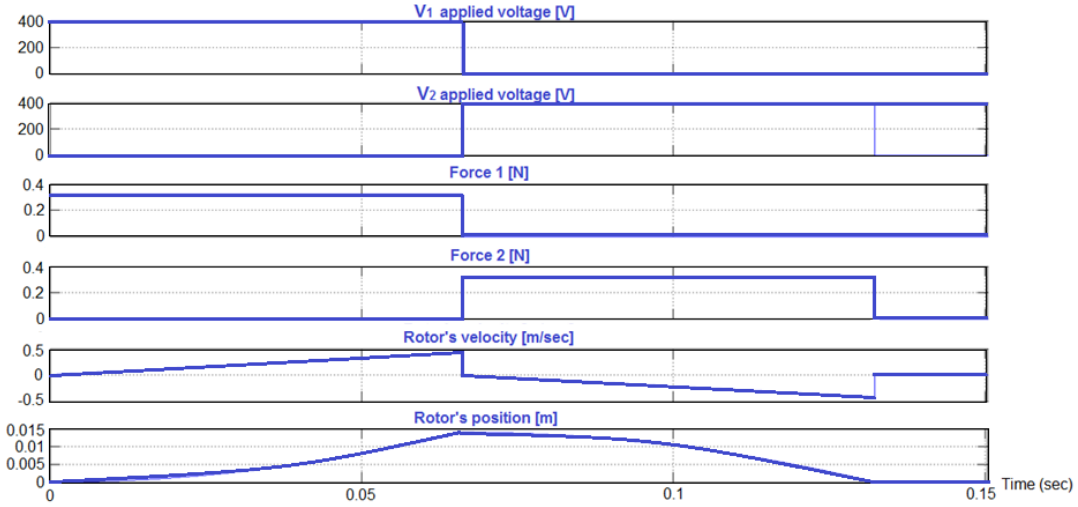

Fig. 4. The applied voltages V1 and V2, the generated forces, the rotor's velocity and position. The rotor moves from zero to +14mm (left direction) and backwards to zero position (right direction)

3.2 Second method: V1 and V2 are sinusoidal voltages

When the sine voltages V1 or V2 are applied to the motor, the generated force (force 1 or force 2) will have squared sine waveform (see eq. (5)). As a result, the obtained velocity profile will have acceleration and deceleration sections.

The operation principle is shown for the case when the V1 and V2 are sinusoidal voltages with amplitude of 400V. The rotor's initial position is zero and it moves to the X=4.2mm position (left direction) and backwards to the zero position (right direction). The simulated V1 and V2 voltages versus the generated forces, rotor's velocity and position profiles are shown in Fig. 5. It can be seen that application of sinusoidal voltages smoothes the velocity profile: its shape is sinusoidal and has acceleration and deceleration sections. When the voltage is applied to the motor, it gradually accelerates and when it approaches to its destination position (X=4.2mm for the left move and X=0

for the right move), it gradually slows down until full stopping. Fig. 6 shows simulated V1 and V2 sinusoidal voltages versus the generated forces, rotor's velocity and position for the case when the rotor's initial position is zero and it moves to the X=4.2mm position (left direction), stops for 0.01sec (delay) and returns backwards to the zero position (right direction).

Application of sinusoidal voltages reduces mechanical jerk and mechanical stresses on the motor. However, in comparison to the cases of DC voltages application, the rotor's velocity and acceleration are limited. Another disadvantage is that initial generated force is zero. Therefore, this method should not be used for starting relatively heavy loads.

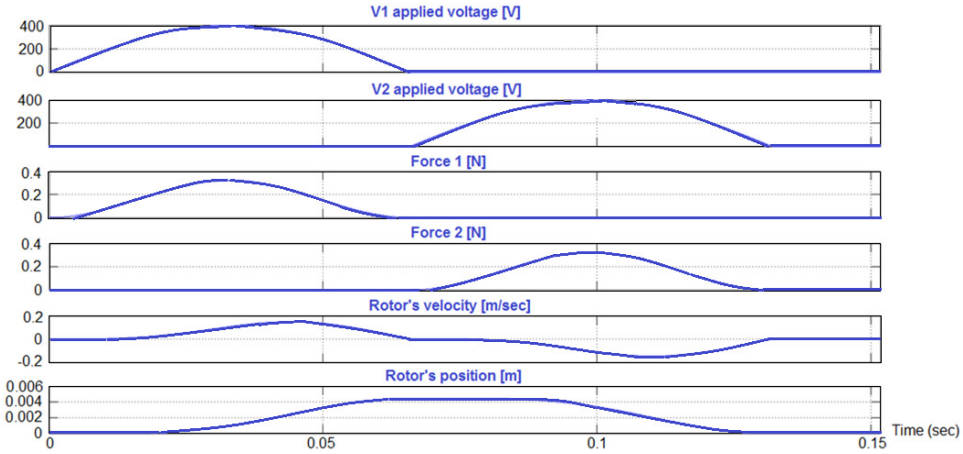

Fig. 5. The applied sinusoidal voltages V1 and V2, the generated forces, the rotor's velocity and position. The rotor moves from zero to +4.2mm (left direction) and backwards to zero position (right direction)

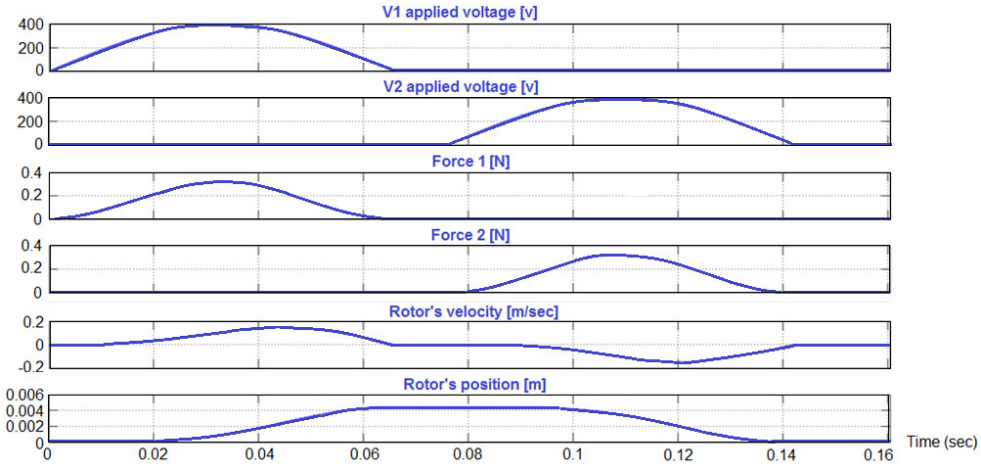

Fig. 6. The applied sinusoidal voltages V1 and V2, the generated forces, the rotor's velocity and position. The rotor moves from zero to +4.2mm (left direction) and backwards to zero position (right direction)

3.3 Third method: V1 and V2 are saw-tooth voltages

The saw-tooth voltages V1 and V2 with amplitude of 400V voltages are applied to the motor. The rotor's initial position is zero and it moves to the X=2.8mm position (left direction) and backwards to the zero position (right direction). The simulated V1 and V2 voltages versus the

generated forces, rotor's velocity and position are shown in Fig. 7. It can be seen that application of saw-tooth voltages generates relatively high starting force. Therefore, this method can be used for starting the motor with relatively high loads. However, the force decays while the rotor approaches its destination position.

Similar to the case of sinusoidal voltages, the velocity profile has acceleration and deceleration sections. When the rotor approaches its destination position, X=2.8mm for the left move and zero for the right move, it gradually slows down until full stopping. As a result, the mechanical stresses on the motor are reduced.

As it was shown, different voltage waveforms can be applied to the motor and each has its advantages and disadvantages.

The voltage waveforms can be easily combined together in order to obtain desired force, velocity and position profiles.

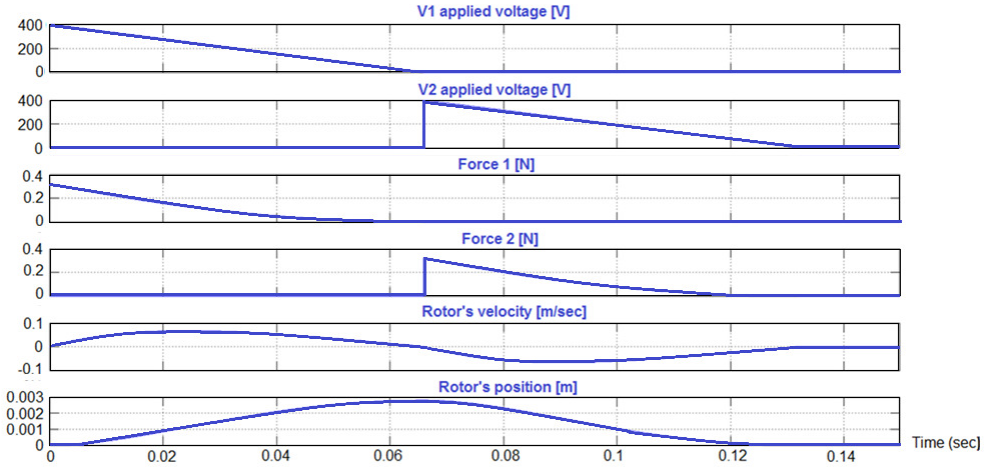

Fig. 7. The applied saw-tooth voltages V1 and V2, the generated forces, the rotor's velocity and position. The rotor moves from zero to +2.8mm (left direction) and backwards to zero position (right direction)

IV. CONCLUSIONS

The new type of linear electrostatic motor was presented. The proposed motor is operated on a principle of the electric field effect. The motor can generate relatively high force on the rotor due to implementation of new dielectric materials with relatively high electric permittivity of $\varepsilon_r = 1.7*10^4$.

The first significant advantage of the proposed motor is a simple structure that simplifies the production process and reduces motor's price.

Furthermore, the proposed motor has advanced motion control options that allow precise control of velocity and position profiles. Extensive simulation results of the proposed motor for different control modes were presented and analyzed.

In the first control method DC voltages V1 and V2 are applied to the motor. This control method is preferable in the cases when fast acceleration and high speed are required. Additional advantage is relatively high starting force of the motor. The disadvantage is that immediate stopping of the rotor can cause mechanical damage to the motor.

In the second control method sine voltages V1 and V2 are applied to the motor. The advantages of this method are relatively small mechanical jerk and mechanical stresses on the motor. The disadvantages are limited rotor velocity and acceleration. Another disadvantage is that initial generated force is zero. This method is not preferable for starting relatively heavy loads.

In the third control method saw-tooth voltages V1 and V2 are applied to the motor. The application of saw-tooth voltages generates relatively high starting force. Therefore, this method can be used for starting the motor with relatively high loads. Additional advantages of this method are relatively small mechanical jerk and mechanical stresses on the motor.

The voltage waveforms can be easily combined together in order to obtain desired force, velocity and position profiles. Moreover, closed loop control can be easily applied to the motor. By using the proposed methods, the motor can be used in optics, mechatronics and robotic systems, where precise motion control is required.

REFERENCES

[1] A. Shenkman, A New Type of Electrostatic Capacitor motor, Journal of the Association of Engineers & Architects in Israel, 1885.

[2] Moore A.D., Electrostatics and its Applications, John Wiley & Sons, 1973, 145-133.

[3] Toshiki Niino, Dual Excitation Electrostatic Stepper Motor, Electrical Engineering in Japan, vol. 119, no. 3, 1997, 94-103.

[4] R. Moser, L. Sache, A. Cassat, T. Higuchi and H. Bleuler, Advances in Precise Positioning Using the Electrostatic Glass Motor, IEEE Trans. Ind. Appl., vol. 41, no. 4, 2005, 972-977.

[5] M. Modabberifar, A. Yamamoto and T. Higuchi, An electrostatic induction actuator for dielectric sheet conveying, IEEE/ASME International Conference on Advanced Intelligent Mechatronics, 2010, 551-556.

[6] R. Saito, T. Hosobata, A. Yamamoto and T. Higuchi, A Resonant Electrostatic Induction Motor with Piezoelectric Elements as Inductors Connected to its Slider Electrodes, IEEE/RSJ International Conference on Intelligent Robots and Systems, 2012, 622-627.

[7] N. Yamashita, A. Yamamoto, M. Gondo, and T. Higuchi, Evaluation of an Electrostatic Film Motor Driven by Two-Four-Phase AC Voltage and Electrostatic Induction, IEEE International Conference on Robotics and Automation, 2007, 1572-1577.

[8] M. Rajenda, A. Yamamoto, T. Oda, H. Kataoka, Motion Generation in MR Environment Using Electrostatic Film Motor for Motion-Triggered Cine-MRI, Trans. Mechatronics, vol. 13, no.3, 2008, 278-285.

[9] Z. Zhang, M. Gondo, N. Yamashita, A. Yamamoto and T. Higuchi, Design and Control of a Fish-like Robot Using an Electrostatic Motor, International Conference on Robotics and Automation, 2007, 974-979.

[10] Z. Zhang, K. Machita, A. Yamamoto and T. Higuchi, Development of a three-phase high-voltage driving system for thin and flexible film motors, ICEMS 2010, 2010, 726-731.

[11] K. Hameyer, R. Belmans, Design of very small electromagnetic and electrostatic micro motors, International Conference on Electric machines and Drives, 1997, TB2/11.1 - TB2/11.3.

[12] D. Yazdani, A. Bakhshai, G. Joos, A Space Vector Classification Technique for MEMS Electrostatic Six-Phase Induction Micro-motors, IECON 2006, 2006, 2303-2306.

[13] Y. Tang, S. X. Chen, T. S. Low, Micro electrostatic actuators in dual-stage disk drives with high track Density, ICSENS 2002, 2002, 1746-1750.

[14] R. Yeh, S. Hollar, K. S. J. Pister, Single mask, large force, and large displacement electrostatic linear Inchworm motors, Journal of Micro-Electromechanical Systems, 2002, 330-336.

[15] E. Serajlik, E. Berenschot, N. Tas, H. Fujita, G. Krijnen, High performance bidirectional electrostatic inchworm motor fabricated by trench isolation technology, International Conference on Solid State Sensors, Actuators and Microsystems, vol. 1, 2005; 53-56.

[16] L. Parrate, G. Racine, N. F. Rooij, E. Bornand, A novel comb-drive electrostatic stepper motor", International Conference on Solid State Sensors, Actuators and Microsystems, 1991, 886-889.

[17] M. Kiang, O. Solgaard, R. S. Muller, Y. Lau, Surface-micro-machined electrostatic-comb driven scanning micro-mirrors for barcode scanners, MEMS 96, 1996, 192-197.

[18] W. C. Tang, M. G. Lim, R. T. Howe, Electrostatic Comb Drive Levitation and Control Method, Journal of Micro-Electromechanical Systems, 1992, 170-178.

[19] K. Suzumori, K. Hori, Micro electrostatic wobble motor with toothed electrodes, MEMS 97, 1997, 227-232.

[20] L. Parrate, G. Racine, N. F. Rooij, E. Bornand, A rigid ring electrostatic harmonic wobble motor with axial field, International Conference on Solid State Sensors, Actuators and Microsystems, 1991, 890-893.

[21] Sanjay Paliwal and H.Chandra, “Investigation of Particulate Control in Thermal Power Plant using Electrostatic Precipitator”, International Journal of Mechanical Engineering & Technology (IJMET), Volume 4, Issue 3, 2013, pp. 149 - 154, ISSN Print: 0976 – 6340, ISSN Online: 0976 – 6359.

[22] Vivek singh and Dr. A.C. Tiwari, “Performance Analysis of Electrostatic Precipitator in Thermal Power Plant”, International Journal of Mechanical Engineering & Technology (IJMET), Volume 3, Issue 2, 2012, pp. 431 - 436, ISSN Print: 0976 – 6340, ISSN Online: 0976 – 6359.